

Modeling the Effect of Curing Pressure on the Viscosity Evolution of Oilwell Cement

Xueyu Pang, Pauline A. Otieno, and Gary P. Funkhouser, Halliburton

Copyright 2014, AADE

This paper was prepared for presentation at the 2014 AADE Fluids Technical Conference and Exhibition held at the Hilton Houston North Hotel, Houston, Texas, April 15-16, 2014. This conference was sponsored by the American Association of Drilling Engineers. The information presented in this paper does not reflect any position, claim or endorsement made or implied by the American Association of Drilling Engineers, their officers or members. Questions concerning the content of this paper should be directed to the individual(s) listed as author(s) of this work.

Abstract

During the cementing operations of oil and gas wells, the high pressure encountered down hole is known to accelerate the cement hydration rate, especially during early stages. It is important to understand the effect of pressure on evolution of various properties of oilwell cement. In this study, the effect of curing pressure (up to 20,000 psi) on viscosity/consistency evolution of different types of oilwell cement was investigated by using pressurized consistometers. A previously proposed scale factor model for simulating the effects of curing temperature and pressure on cement hydration kinetics under isothermal and isobaric test conditions is further developed to model the viscosity evolution of cement slurries under variable temperature and pressure conditions. New and historical test data of different types of cement with a variety of temperature and pressure test schedules were analyzed using the proposed model. The fitted results indicate that, with similar temperature test schedules, the viscosity evolution of a given cement slurry as a function of time at different curing pressures can be accurately predicted using only test results at a reference pressure condition (such as atmospheric) and two chemical kinetic parameters of the cement, namely the activation energy and activation volume. The apparent activation volume, determined based on viscosity evolution test data at relatively low pressures ($\leq 6,500$ psi) and near ambient temperature (77 to 80°F), ranges from -37.5 to -32 cm^3/mol for different types of cement, which appears to decrease with both increasing temperature and increasing pressure.

Introduction

Increased demand for hydrocarbon energy is gradually leading to the depletion of relatively shallow, easy-to-recover reserves. Frequently, wells of greater depth with high-pressure/high-temperature (HP/HT) conditions are encountered. These extreme conditions present numerous challenges during well cementing operations. For example, the property evolution of oilwell cement is strongly dependent on curing conditions. Curing temperature has a particularly strong effect on the cement hydration rate¹ and can lead to significant changes in the long-term properties of oilwell cements at temperatures above 230°F due to phase changes of cement hydration products^{2,3}. The curing pressure does not appear to

have a significant impact on long-term properties of oilwell cements after setting⁴. However, it has been shown that curing pressure accelerates early cement hydration in a similar manner to curing temperature, with a relatively small magnitude^{1,5}. As the maximum well pressure encountered in the field continues to increase, it is important to gain a better understanding on the influence of curing pressure on the property evolution of oilwell cement.

As a result of the production and accumulation of cement hydration products, viscosity of a cement slurry generally increases with time after mixing until the slurry transforms into a solid (setting). During the cementing operation of a well, it is essential for the cement slurry to remain as a pumpable fluid until placement. Premature setting can have serious consequences and even result in complete abandonment of a well. Conversely, a long setting time increases the potential for gas or fluid flow into the cement sheath and/or unproductive wait-on-cement (WOC) time, hence increasing the operational cost. For a given oilwell cement slurry, its viscosity evolution and setting time are strongly dependent upon curing conditions, primarily downhole temperature and pressure. The viscosity evolution of an oilwell cement slurry is typically measured in the laboratory by HP/HT consistometers at simulated downhole curing conditions. The viscosity is reported in Bearden consistency units (Bc), and the limit of pumpability (LOP) beyond which the slurry is considered too viscous to pump is approximately 70 to 100 Bc. The time required for a cement slurry to reach the LOP is known as the thickening time.

The effect of curing temperature and pressure on the thickening time of oilwell cement slurries has been successfully modeled by Scherer et al.⁶, where a boundary nucleation and growth model (or the Avrami-Cahn model) was used to simulate the early hydration progress of cement. Considering that many details of the cement hydration mechanism are still not clearly understood today, whether the boundary nucleation and growth model is a true representation of the cement hydration process is still a subject of considerable debate. Additionally, application of such a model is difficult for users without proper knowledge of cement hydration kinetic theories. Recently, a much more straightforward model for simulating the effect of curing temperature and pressure on the cement hydration progress

was introduced by Pang et al.^{1,5}, where the hydration kinetics of cement is represented by an undefined function, bypassing the uncertainties associated with the cement hydration mechanism. The model has been previously applied to predict the evolutions of chemical shrinkage¹ and heat of hydration⁵ of oilwell cement. In this study, the possibility of using the model to predict the viscosity evolution of oilwell cement slurries at different curing conditions by assuming that slurry viscosity has a direct correlation with the degree of hydration of cement is explored. Such a model allows the prediction of not only the thickening time, but also the complete slurry viscosity evolution profile as a function of time.

Theoretical Background

The theoretical framework for modeling the effects of temperature and pressure on property evolution of Portland cement under isothermal and isobaric curing conditions has been developed in a previous study¹. The two primary goals of this study are to expand the model to include variable temperature and pressure curing conditions and to test the applicability of the model for the viscosity property of oilwell cement.

For tests performed under isothermal and isobaric conditions, the effects of temperature and pressure on the property evolution of cement-based materials can be represented by a simple scale factor, provided that the property can be assumed to have a direct correlation with the degree of hydration of cement¹. For example, assuming that the viscosity evolution of a cement slurry at a reference temperature, T_r , and pressure, P_r , is represented by Eq. 1.

$$\eta = \eta_{T_r, P_r}(t) \quad (1)$$

Then the viscosity evolution at arbitrary temperature, T , and pressure, P , can be represented by Eq. 2.

$$\eta = \eta_{T, P}(t) = \eta_{T_r, P_r}(C \cdot t) \quad (2)$$

where C is a scale factor that describes the cement hydration rate change compared to the reference condition because of a curing condition change. For example, a scale factor of 2 means that the hydration rate is doubled, while a scale factor of 0.5 means that the hydration rate is reduced in half. When modeling the main hydration of cement (first few days), it is often necessary to introduce an offset time parameter to generate better fits to hydration kinetics test data^{1,5,7}. The cause of such an offset is not clear. It might be attributed to experimental artifacts (slurries not mixed at in-situ temperature and pressure conditions), or that cement hydration follows a different mechanism during the very early stage (i.e., the preinduction period, or the initial reaction). The magnitude of the time offset is usually very small and often equals zero for tests conducted at the same temperature and variable pressures. For the purpose of modeling early-age properties, such as cement slurry viscosity, it is best to leave out the offset time parameter, which is unpredictable. The dependence of the scale factor on curing temperature and pressure can be modeled by Eq. 3¹.

$$C(T_r - T, P_r - P) = \exp\left(\frac{E_a}{R}\left(\frac{1}{T_r} - \frac{1}{T}\right) + \frac{\Delta V^\ddagger}{RT}(P_r - P)\right) \quad (3)$$

where E_a is the apparent activation energy (J/mol), which describes the temperature sensitivity of a chemical reaction; ΔV^\ddagger is the apparent activation volume (m³/mol), which describes the pressure sensitivity of a chemical reaction; R is the gas constant (8.314 J/(mol·K)); T and P are the absolute temperature (K) and pressure (Pa) of an arbitrary curing condition, while T_r and P_r are the temperature (K) and pressure (Pa) of the reference curing condition.

As discussed in a previous study⁸, the scale factor model presented here is very similar to the maturity method⁹ for estimating the effect of curing temperature on the strength evolution of concrete in the construction industry. It is convenient to extend the maturity concept to include oilwell cement for better understanding and application of the scale factor model. Maturity can be defined as the extent of the development of a property of a cementitious mixture, and equivalent age can be defined as the amount of time required at a reference curing condition (T_r, P_r) to produce a maturity equal to the maturity achieved by a curing period at curing conditions (T, P) different from the reference. The maturity method assumes that the property evolution of a cementitious mixture as a function of equivalent age is the same for all curing conditions. The equivalent age (t_r) at the reference curing condition can be computed numerically using Eq. 4.

$$t_r = \sum C \cdot \Delta t = \sum \exp\left(\frac{E_a}{R}\left(\frac{1}{T_r} - \frac{1}{T(t)}\right) + \frac{\Delta V^\ddagger}{RT(t)}(P_r - P(t))\right) \cdot \Delta t \quad (4)$$

where $T(t)$ and $P(t)$ are the average temperature and pressure during time interval Δt , respectively. Eq. 4 reduces to $t_r = Ct$ for isothermal and isobaric curing conditions (i.e., constant T and P). In reality, however, the curing temperature and pressure of oilwell cements are almost always functions of time during the process that they are mixed on the surface and pumped downhole.

Calculation of the equivalent age can be used to predict the property evolution of a cement mixture at an arbitrary curing condition based on the experimental data of a single test at another arbitrary curing condition. The following example is provided to further illustrate details of the modeling process. Suppose one has the viscosity evolution test data of a slurry at curing condition A , with temperature $T_A(t)$ and pressure $P_A(t)$, and one needs to predict the viscosity evolution of the same slurry at curing condition B , with temperature $T_B(t)$ and pressure $P_B(t)$. Using Eq. 4, and test data at curing condition A , one can first obtain the viscosity or consistency as a function of equivalent age (t_r) at a reference isothermal and isobaric condition (see **Table 1** for numerical representation). Similarly, using Eq. 4 and the known temperature and pressure functions at curing condition B , the corresponding equivalent age (t'_r) can also be calculated at the same reference condition (see **Table 2** for numerical representation). As the viscosity evolution should follow the same function at the same

reference condition (i.e., $\eta'(t'_r) \equiv \eta(t_r)$), the unknown η' can be calculated as a function of t'_r by linear interpolation using test data of the known η as a function of t_r .

While the model presented is applicable for a wide range of pressure changes, it is only applicable for small temperature changes because temperature itself significantly influences cement slurry viscosity. This will be discussed in more detail further in the paper.

Table 1—Test Data at Curing Condition A

Real Time (t_A)	$T_A(t_A)$	$P_A(t_A)$	Equivalent Age (t_r)	Consistency (η)
t_{A1}	T_{A1}	P_{A1}	t_{r1}	η_1
...
t_{Ai}	T_{Ai}	P_{Ai}	t_{ri}	η_i
$t_{A(i+1)}$	$T_{A(i+1)}$	$P_{A(i+1)}$	$t_{r(i+1)}$	η_{i+1}
...
t_{An}	T_{An}	P_{An}	t_{rn}	η_n

Table 2—Predicted Results at Curing Condition B

Real Time (t_B)	$T_B(t_B)$	$P_B(t_B)$	Equivalent Age (t'_r)	Consistency (η')
t_{B1}	T_{B1}	P_{B1}	t'_{r1}	η'_1
...
t_{Bi}	T_{Bi}	P_{Bi}	t'_{ri}	η'_i
$t_{B(i+1)}$	$T_{B(i+1)}$	$P_{B(i+1)}$	$t'_{r(i+1)}$	η'_{i+1}
...
t_{Bn}	T_{Bn}	P_{Bn}	t'_{rn}	η'_n

Experimental Program

The effect of the curing condition on the viscosity evolution of a white cement and a Class H cement has been investigated in a previous study, test data of which will be revisited for validation of the model proposed here. Two other types of oilwell cement, API Class A and Class C cements, were tested in this study to further study the dependency of test results on cement chemical or physical properties. **Table 3** presents the main compound compositions of these cements derived from oxide analysis test results using the Bogue calculation method¹⁰, as well as powder X-ray diffraction (XRD) using the accompanying Rietveld refinement¹¹. The estimated primary phase compositions, by the two different methods, agree reasonably well with one another, except for the C_3A contents. The XRD results appear to show no diffraction peaks associated with C_3A and higher C_4AF contents in both cements. The particle size distributions of the cements were measured by the laser scattering technique using a dry dispersion method. **Fig. 1** illustrates the average test results. The median particle sizes for Class A and Class C cements were 23.1 and 11.3 μm , respectively, while their calculated specific surface areas (assuming spherical particles and a density of 3150 kg/m^3 for cement) were 280 and 418 m^2/kg , respectively.

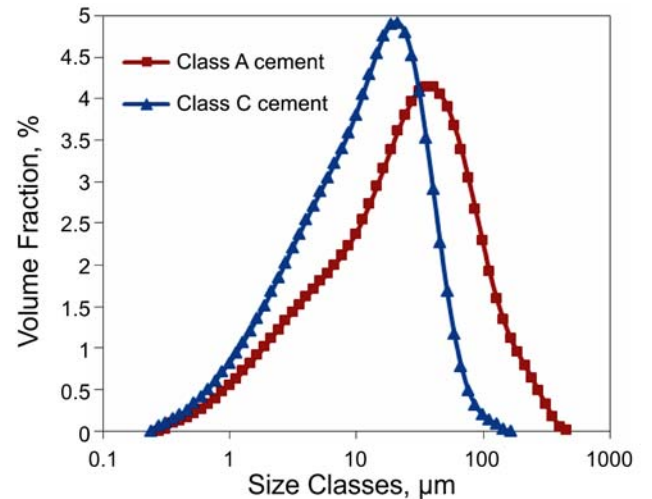


Fig. 1—Particle size distributions of Class A and C cements.

Table 3—Estimated Main Compound Compositions (by Mass Percentage) of the Different Cements

Cement	Method	C_3S	C_2S	C_3A	C_4AF	$CaSO_4$	Free Lime
A	Bogue	55.3	17.5	10.0	8.5	5.2	1.4
	Rietveld	63.3	18.3	0	12.8	5.5 ^a	—
C	Bogue	70.5	3.4	5.9	11.1	5.6	0.76
	Rietveld	69.1	7.7	0	16.1	7.1 ^a	—

^aGypsum ($CaSO_4 \cdot 2H_2O$) content

All slurries were prepared in a Waring blender at room temperature using deionized water and cement only (i.e., neat slurries with no admixtures) according to the procedures outlined in API RP 10B¹². To reduce the variability of the initial slurry temperature, the mixing water is allowed to reach an equilibrium temperature with the laboratory (approximately 70°F) before mixing. A water-to-cement (w/c) mass ratio of 0.45 was used for the Class A cement, while a w/c ratio of 0.55 was used for the Class C cement. The densities of the resultant Class A and Class C cement slurries were 15.8 and 15 lbm/gal , respectively. Thickening time tests were performed according to the procedures outlined in API RP 10B¹² at a constant temperature of approximately 77°F and different pressures. For each class of cement, four tests were conducted at curing pressures of 300, 6,500, 13,000, and 19,500 psi, respectively, using a ramp time of 5 min to create near isobaric conditions, while one additional test was conducted using a much slower ramp rate (10,000 psi/hr for Class A cement and 5,000 psi/hr for Class C cement) to a final pressure of 19,500 psi.

Test Results and Discussion

Test Data Preprocessing

Thickening time tests of oilwell cement are usually conducted in HP/HT consistometers. Because of the relatively large size of the sample (approximately 0.475 liter), it is often

difficult to precisely control the sample temperature. Temperature fluctuations of a few degrees are typical, especially toward the end of the test when the heat released from cement hydration begins to accelerate. A slight temperature gradient may also exist within the sample. **Fig. 2** illustrates the slurry temperature fluctuations of the tests in this study, which were conducted with the coolant off. Although pressure control is generally more uniform and accurate, minor deviations from the test schedule are also possible, especially during the initial pressurization period. Hence, tests conducted using HP/HT consistometers are not strictly isothermal or isobaric. However, test data can be modified/pre-processed by calculating the equivalent age for true isothermal and isobaric curing conditions, which are necessary for the derivation of the chemical kinetic parameters (i.e., activation energy E_a and activation volume ΔV^\ddagger). **Fig. 3** provides an example of the thickening time test of Class A cement cured at 77°F and 13,000 psi before and after converting to isothermal and isobaric conditions. The conversion of the actual curing time/age to equivalent age is achieved by using the real-time slurry temperature and pressure data and the process described in **Table 1**. As Eq. 4 indicates, because the chemical kinetic parameters are also needed for the computation of equivalent age, they can only be solved iteratively. It appears difficult to obtain the accurate activation energy of a cement from thickening time test data. In this study, the activation energy of the cement is derived from isothermal calorimetry tests using the peak hydration rate method⁷, while the activation volume of the cement is solved iteratively based on thickening time test data. Because the pressure deviations (from a targeted isobaric condition) are usually very small, one iteration appears to be sufficient to obtain the final estimate of the activation volume.

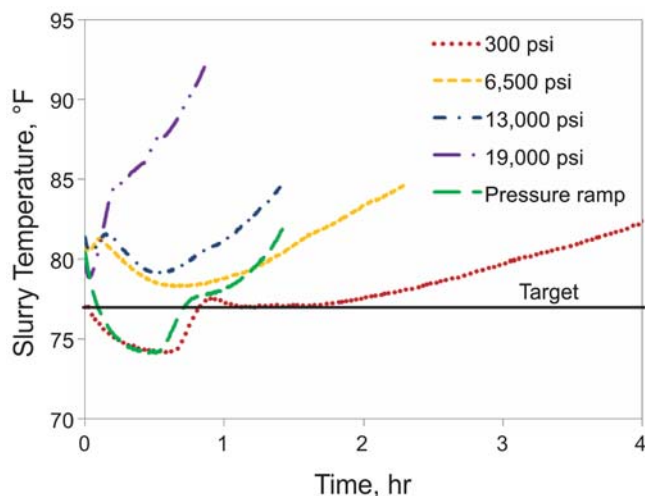


Fig. 2—Target temperature vs. actual slurry temperature evolution of Class A cement at different curing pressures.

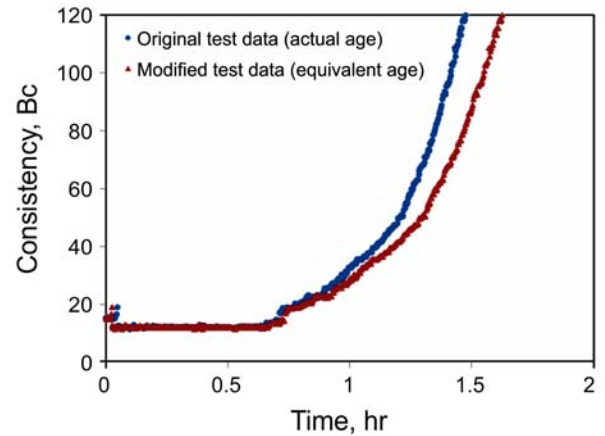


Fig. 3—Test data of Class A cement cured at 77°F and 13,000 psi before and after converting to isothermal and isobaric conditions

Class A Cement

Fig. 4 illustrates the viscosity evolution profiles of Class A cement conducted at 77°F and different curing pressures. An activation energy of 42 kJ/mol, as derived from isothermal calorimetry tests, was used to convert test data to true isothermal conditions. It is apparent that the consistency of the cement slurry increases at much faster rates at elevated curing pressures. The measured thickening time was reduced from 3.5 hr at 300 psi to 0.95 hr at 19,500 psi. The slurry tested with a pressure ramp of 10,000 psi/hr had a thickening time of approximately 1.7 hr.

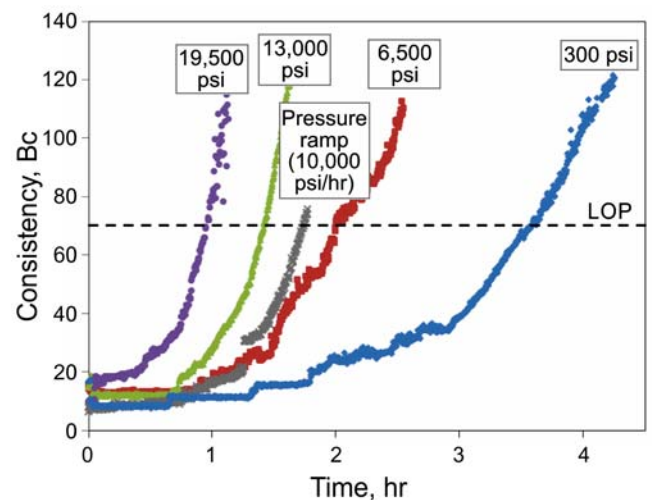


Fig. 4—Viscosity evolution of Class A cement cured at 77°F and different curing pressures.

Based on the scale factor model presented in this study, the viscosity evolution of the cement at different curing conditions should overlap when plotted as a function of equivalent age. As shown in Eq. 4, for isothermal and isobaric tests, the equivalent age can be calculated simply by multiplying the time by a factor of C . The test data presented

in Fig. 4 are replotted as functions of equivalent age using 77°F and 300 psi as a reference curing condition in Fig. 5, which show very good agreement among different tests. However, it appears that the activation volume used for computing the equivalent age must vary for different curing pressures to produce the best agreements. This will be discussed in further detail later during this study. Fig. 6 illustrates that one can use the thickening time test data at one curing condition (i.e., 77°F and 300 psi in this case) to predict test results at other curing conditions based on the model presented in this study.

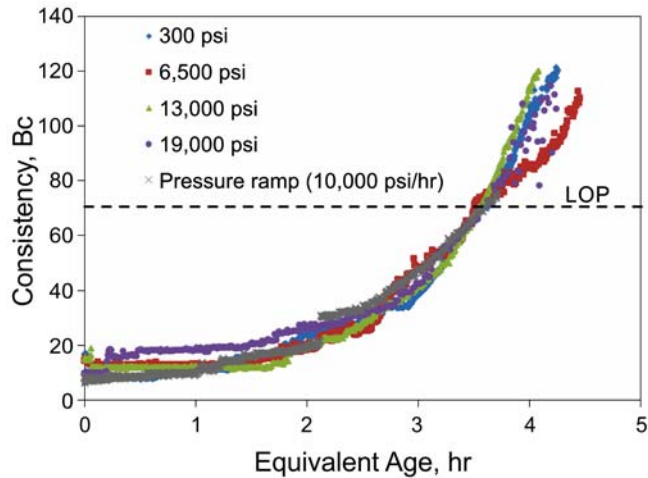


Fig. 5—Viscosity evolution of Class A cement as a function of equivalent age using 77°F and 300 psi as a reference curing condition.

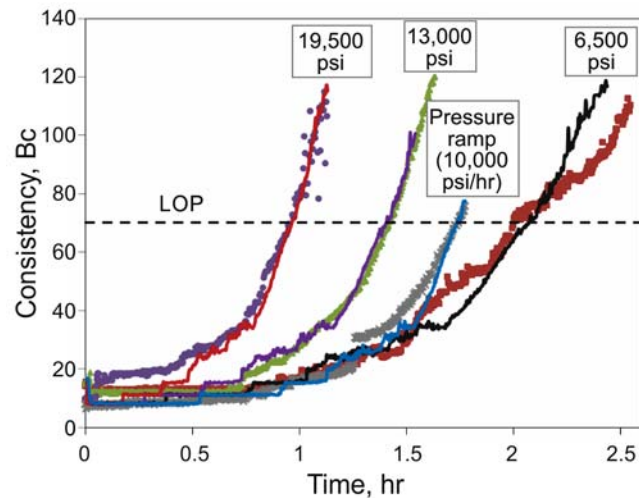


Fig. 6—Experimental and predicted viscosity evolution of Class A cement cured at 77°F and different curing pressures (symbols represent experimental data and solid lines represent model predictions).

Class C Cement

Similar to the test results of Class A cement, the viscosity evolution of Class C cement at different curing conditions also showed very good agreement when plotted as functions of the equivalent age. Fig. 7 illustrates the computed test results using 77°F and 300 psi as a reference curing condition. The activation volume that provides the best fit to the test results also varies with curing pressure. As discussed previously, any test can be used to predict test results at other arbitrary curing conditions. Fig. 8 illustrates that one can use the thickening time test data at 77 °F and 19,500 psi to predict test results at other curing conditions based on the model presented in this study. For this particular cement slurry, the measured thickening time was reduced from 4.4 hr at 300 psi to 1.2 hr at 19,500 psi. The slurry tested with a pressure ramp of 5,000 psi/hr had a thickening time of approximately 2.5 hr.

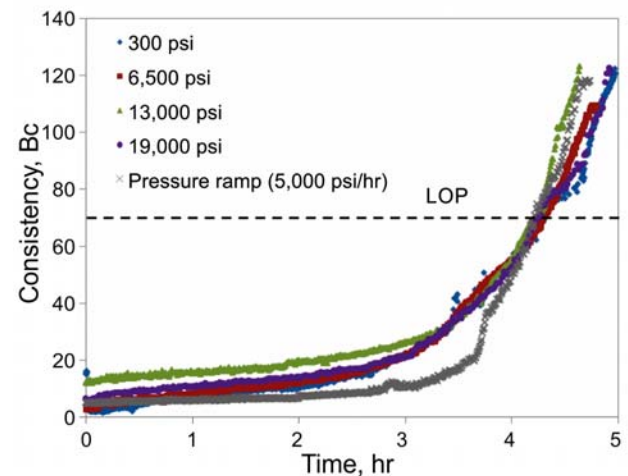


Fig. 7—Viscosity evolution of Class C cement as a function of equivalent age using 77°F and 300 psi as a reference curing condition.

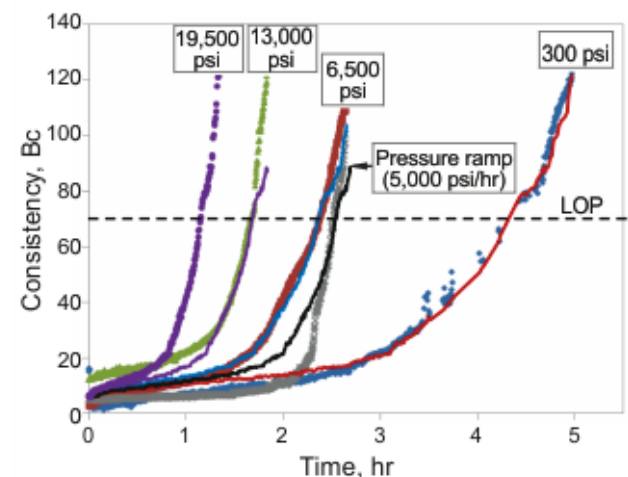


Fig. 8—Experimental and predicted viscosity evolution of Class C cement cured at 77°F and different pressures (symbols represent experimental data and solid lines represent model predictions).

Lehigh White Cement (Test Data from Reference 6)

Scherer et al.⁶ performed a similar study to the one , where the thickening time of a white cement with a w/c ratio of 0.46 was tested at 80°F and different curing pressures. Test data were analyzed with the model presented in this study. **Fig. 9** illustrates that the viscosity evolution of the cement at elevated curing pressures can be predicted using the test results at atmospheric pressure with excellent accuracy. Similar to previous observations, the activation volume that provides the best fit in the test results also varies with curing pressure. For this particular cement, the measured thickening time was reduced from 3.7 hr at atmospheric pressure to 0.75 hr at 20,000 psi.

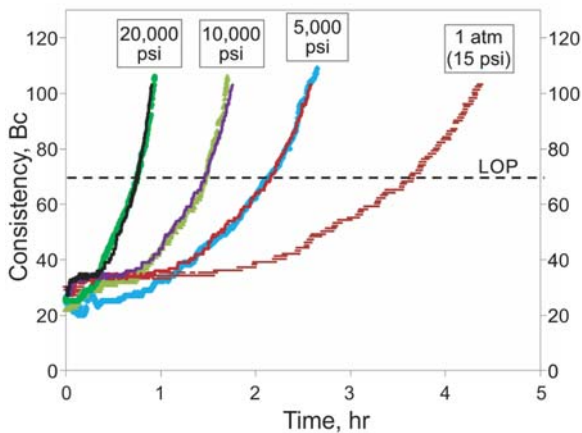


Fig. 9—Experimental and predicted viscosity evolution of Lehigh white cement cured at 80°F and different pressures (symbols represent experimental data and solid lines represent model predictions).

Additionally, the thickening time of the white cement was also tested at different curing temperatures⁶. Because it is nearly impossible to perform temperature jumps with HP/HT consistometers, the curing temperature was ramped from the ambient condition to different targets (135, 140, and 146°F) in approximately 41 min. **Fig. 10** compares the experimental and predicted viscosity evolution test results at different curing temperatures using the 140°F target temperature test results and an activation energy of 33.8 kJ/mol. While the viscosity evolution at 135 and 146°F can be predicted with reasonable accuracy, the prediction for the test results at the 80°F isothermal curing condition deviated significantly from experimental data. This is primarily because the model assumption that slurry viscosity has a direct correlation with the degree of hydration of cement is no longer valid for large temperature changes. Unlike pressure, temperature is known to have a significant effect on the viscosity of water¹³, which is one of the main components of the cement slurry. The thickening time at 80°F can be predicted with better accuracy if an activation energy of 42 kJ/mol is adopted, but the viscosity evolution profiles clearly no longer match each other.

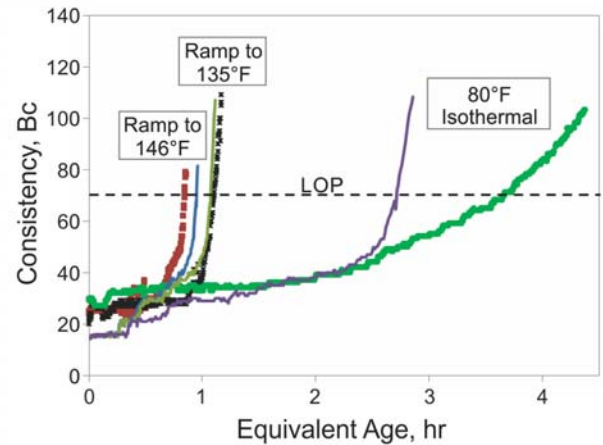


Fig. 10—Experimental and predicted viscosity evolution of Lehigh white cement at different curing temperatures and atmospheric pressure (symbols represent experimental data and solid lines represent model predictions).

All test data presented until this point were obtained at either constant temperature or constant pressure curing conditions. In reality, as oilwell cement is pumped downhole, it is likely to be subjected to a gradual increase in both temperature and pressure. The Lehigh white cement was also tested using both temperature and pressure ramps⁶ to simulate such conditions. A series of tests were performed using the same target temperature (135°F) and different target pressures (1 atm, 4,900, 10,000, and 20,000 psi). **Fig. 11** illustrates that the test results at different pressure conditions can be predicted accurately using the ramp at 135°F and 4,900 psi test results in conjunction with an activation energy of 33.8 kJ/mol and an activation volume that varies with the target pressure. The thickening time was reduced from 1.1 hr at atmospheric pressure to 0.7 hr at 20,000 psi target pressure.

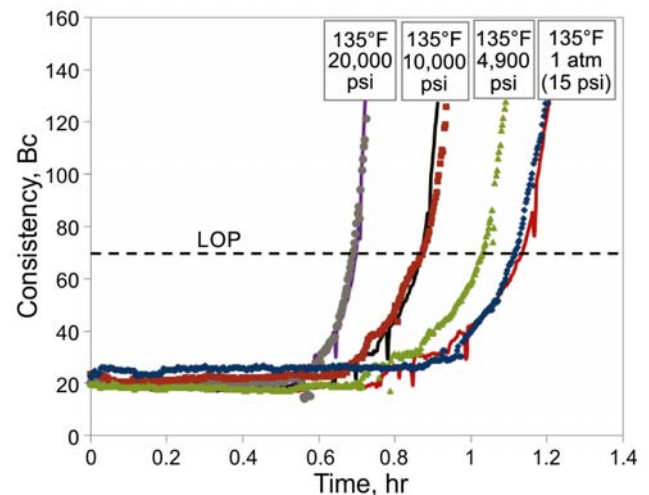


Fig. 11—Experimental and predicted viscosity evolution of Lehigh white cement with both temperature and pressure ramps (symbols represent experimental data, and solid lines represent model predictions).

Apparent Activation Volume of Cement

As discussed in previous studies, cement hydration is a complex process that involves the simultaneous reactions of several different phases. The kinetics model presented in this study is only an approximation for modeling cement property evolution. The activation volume of cement in the model does not describe a single reaction process and is often called the apparent activation volume. It represents the pressure sensitivity of the overall cement hydration reaction, with a larger absolute value corresponding with higher pressure sensitivity. **Table 4** lists the apparent activation volumes of different types of cement for different curing conditions, which were obtained by comparing test results at a specific curing condition with test results at near ambient conditions to achieve the best agreements. **Table 4** also includes the corresponding scale factors obtained for different isobaric tests. At near ambient temperature, the apparent activation volume appears to vary little among different types of cement, although white cement is found to have a slightly higher apparent activation volume. Test results of all cements indicate a decrease in the magnitude of apparent activation volume with increasing curing pressure (approximately 20 to 30% for the range studied). An even more significant decrease is observed with increasing curing temperature for the white cement. A previous study based on the isothermal calorimetry test data of Class G and Class H cements also suggests that the apparent activation volume of cement decreases with increasing curing temperature, but at a much slower rate compared to that determined in this study. These results suggest that the hydration rate of cement becomes less sensitive to pressure changes either at elevated curing temperatures or pressures.

One of the primary advantages of the scale factor model is that it is very straightforward to understand and can be conveniently used as a rule-of-thumb estimate for the effect of curing pressure on the cement hydration rate and resultant cement property evolution, such as the viscosity evolution as discussed here. **Fig. 12** illustrates the scale factors obtained for different cements at different isobaric curing pressures using the ambient condition as a reference. It appears that the dependence of the scale factor on curing pressure can also be fitted by a simple linear model instead of the chemical kinetics model presented in Eq. 4. Just as the best fit activation volume varies with different cements and different curing pressures, so is the best fit slope of the linear model. Nevertheless, all test data obtained in this study fall within a range bounded by a lower slope of 0.1 and an upper slope of 0.19, which suggests that the cement hydration rate is increased 10 to 19% for every 1,000-psi increase in curing pressure based on the viscosity evolution test results.

Table 4—Apparent Activation Volumes of Different Types of Cement at Different Curing Conditions and Corresponding Scale Factors for Isobaric Tests

Cement	$P_r - P$ (psi)	C	ΔV^{\ddagger} (cm ³ /mol)	$\Delta V^{\ddagger a}$ (cm ³ /mol)
Class A (77°F)	300 to 6,500	1.7	-32	-24.1
	300 to 13,000	2.3	-24	
	300 to 19,500	3.8	-25	
	Constant ramp (10,000 psi/hr)	N/A	-27	N/A
Class C (77°F)	300 to 6,500	1.8	-35	-24.3
	300 to 13,000	2.55	-26.5	
	300 to 19,500	3.8	-25	
	Constant ramp (5,000 psi/hr)	N/A	-28	N/A
White ^b (80°F)	0 to 5,000	1.7	-37.5 ^c	-27.7
	0 to 10,000	2.5	-33 ^c	
	0 to 20,000	4.75	-28 ^c	
White ^b (ramp ^d to 135°F)	Ramp ^d to 4,900 psi	N/A	-13 ^c	N/A
	Ramp ^d to 10,000 psi	N/A	-20 ^c	
	Ramp ^d to 20,000 psi	N/A	-22 ^c	
Class H ^b (ramp ^d to 135°F)	Ramp ^d to 5,000 psi	N/A	-30 ^c	N/A
	Ramp ^d to 10,000 psi	N/A	-30 ^c	
	Ramp ^d to 20,000 psi	N/A	-31 ^c	

^aObtained by linear regression based on isobaric tests

^bTest data from Reference 6

^cAverage of at least two duplicate tests

^dTotal ramp time of 41 min

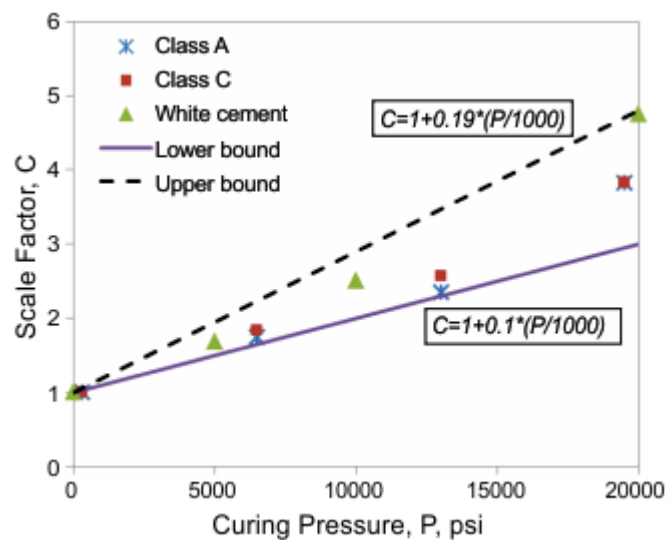


Fig. 12—Scale factor as a function of curing pressure for different types of cement.

Conclusions

The viscosity evolution of several different types of cement under a variety of temperature and pressure curing schedules were investigated in this study. The analysis of new and historical test data supports the following conclusions:

- The rate of viscosity evolution of cement slurry is dramatically increased with increasing curing pressure caused by an increased cement hydration rate.
- The evolution of cement slurry viscosity with similar temperature schedules but significantly different pressure schedules follow a similar profile when plotted as a function of equivalent age for the same reference condition, which allows the modeling of the pressure dependency of cement slurry viscosity evolution.
- The magnitude of the apparent activation volume of cement, which correlates with the pressure sensitivity of the cement hydration rate, decreases with both increasing curing temperature and increasing curing pressure.
- A rule of thumb estimate for the effect of curing pressure on the cement hydration rate indicates a 10 to 19% increase (depending on the cement type and pressure range being considered) for every 1000 psi increase in curing pressure from the atmospheric condition.

Refinement of an Oil Field Cement Blend. Paper presented at the Materials Science and Technology Conference, Columbus, Ohio, USA, 16–20 October.

12. API RP 10B. Recommended Practice for Testing Well Cements, second edition, 2013. Washington, DC, API.
13. Schmelzer, J.W.P., Zanotto, E.D., and Fokin, V.M. 2005. Pressure Dependence of Viscosity. *The Journal of Chemical Physics*. **122** (074511).

References

1. Pang, X., Meyer, C., Darbe, R., and Funkhouser, G.P. 2013. Modeling the Effect of Curing Temperature and Pressure on Cement Hydration Kinetics. *ACI Materials Journal*. v. **110** (2): 137–148.
2. Swayze, M.A. 1954. Effects of High Pressure and Temperatures on Strength of Oil-Well Cements. *Drilling and Production Practice. American Petroleum Institute*. 72–81. API-54-072.
3. Bensted, J. Special Cements. 1998. In *Lea's Chemistry of Cement and Concrete*, fourth edition, ed. P.C. Hewlett. 783–811. Elsevier: Amsterdam.
4. Pang, X. 2011. Effects of Curing Temperature and Pressure on the Chemical, Physical, and Mechanical Properties of Portland Cement. PhD dissertation, Columbia University.
5. Pang, X., Cuello Jimenez, W., and Iverson, B.J. 2013. Hydration Kinetics Modeling of the Effect of Curing Temperature and Pressure on the Heat Evolution of Oil Well Cement. *Cement and Concrete Research*. **54**: 69–76.
6. Scherer, G.W., Funkhouser, G.P., and Peethamparan, S. 2010. Effect of Pressure on Early Hydration of Class H and White Cement. *Cement and Concrete Research*. **40** (6): 845–850.
7. Pang, X., Bentz, D.P., Meyer, C., Funkhouser, G.P., and Darbe, R. 2013. A Comparison Study of Portland Cement Hydration Kinetics as Measured by Chemical Shrinkage and Isothermal Calorimetry. *Cement and Concrete Composites*. **39**: 23–32.
8. Pang, X., Bentz, D.P., and Meyer, C. 2012. Modeling Cement Hydration Kinetics using the Equivalent Age Concept. Paper presented at the 3rd International Symposium on Ultra-High Performance Concrete and Nanotechnology for High-Performance Construction Materials, Kassel, Germany, 7–9 March.
9. ASTM C1074. Standard Practice for Estimating Concrete Strength by the Maturity Method. 2010. West Conshohocken.
10. Bogue, R.H. 1929. Calculation of the Compounds in Portland Cement. *Industrial and Engineering Chemistry, Analytical Edition*. **1** (4): 192–197.
11. Iverson, B., Loghry, R., and Edwards, C.L. 2011. Rietveld